Heliyon 10 (2024) e30297

Contents lists available at ScienceDirect

Heliyon

journal homepage: www.cell.com/heliyon

Research article

Assessment of the effects of climate change on water balance components in the upper Erer subbasin, Ethiopia

Bedasa Abrahim Mummed *, Yilma Seleshi

Addis Ababa University, Addis Ababa Institute of Technology, Ethiopia

A R T I C L E   I N F O

Keywords:
Water balance
Climate change
Scenarios
Historical
Projections
Rainfall
Temperature

A B S T R A C T

Eastern Ethiopia watersheds are located in transition zone from Arid to semi-humid climate and in expanding to westwards the west annual rainfall is highly declining. This paper explains future hydrological response impacts under changing climate using ensemble average of the CORDEX RCMs for historical (1979–2014) and future (2024–2070) periods. The result revels the monthly average temperature varies (0.04–6.25°C) for RCP-4.5, while it varies (0.03–6.59°oC) for RCP-8.5. The monthly average rainfall to be decline by 90.71 mm and rise by 211. 22 mm for RCP-4.5, while it is going to decline by 84.97 mm and rise by 235.62 mm for RCP-8.5. The adjusted SWAT model was used to detect the changes of projected hydrological response from reference period. Balance components of the baseline period was compared to future period. The result shows the change in decrease of annual mean surface flow (4.98 %–5.63 %), groundwater flow (5.63 %–6.68 %), evapotranspiration (2.45 %–2.57 %) and water yield (5.54 %–5.21 %) to be expected from RCP-4.5 to RCP-8.5. The findings of this paper provide valuable assistance to water resource planners by enhancing their comprehension of change in climate effects at local level.

1. Introduction

The global warming contributes the change in surrounding atmosphere by increasing local temperature and variability in rainfall. Globally this situation is expected to affect the hydrological processes [[1–8]]. In recent years, the changing climate effects analysis conducted at different function of water sources worldwide for instance Refs. [7,9–14] indicate that their effect increases water shortage in the system. The increase in temperature and rainfall variability expected in the future [15–18]; [19]] aggravate the water resources stress. Hence, climate change studies are remarkable in the sustainability of water sources and the effects can touch different parts of the world [20,21]. In this regard, less developed countries are probably impacted mostly and Ethiopia stands in the first list [22]. The waters scarcity problem coupled with increasing climate change extremes affect the water supply sources of local communities in eastern Ethiopia. The Upper Erer subbasin of the eastern Ethiopia, which is the proposed and existing water supply sources for Harar town, has been suffering from water scarcity [23,24]. This implies conducting changing climate impact studies in the country used for better understanding of their effect. Today many researchers such as [25–30] rank the importance of water resource challenge by climate change effects. But, most of these analyses were implemented on large basins with coarser data [18]. So, high-resolution data are required to efficiently quantify climate change impacts at local scale. To cope up this problem various institutions developed high resolution climate models such as National Aeronautics and Space Administration (NASA), World Climate Research Program

* Corresponding author.
E-mail address: bedasa.abrahim@aait.edu.et (B.A. Mummed).

https://doi.org/10.1016/j.heliyon.2024.e30297
Received 26 July 2023; Received in revised form 22 April 2024; Accepted 23 April 2024
Available online 26 April 2024

(WCRP) [17,31]. The WCRP generated Coordinated Regional Climate Downscaling Experiment (CORDEX) Regional Climate 4 Models (RCMs) and easily accessible [32].

The CORDEX RCMs can capture at local scale for changing climate studies that could be affected by elevation difference [29, 32–34]. The CORDEX RCMs have been assessed in numerous studies on Africa that have well performance in simulating temperature and precipitation [35–41] are used in this study. The RCMs can be influenced by geographical location and the correctness of climate variables [42]. Using the RCMs data directly for climate models without bias correction make the output unreliable [37,39,41]. The performance of RCMs was strongly represented by the consequence of bias adjustments in RCMs simulation. The CMhyd models that defined as Climatic Model Data for the Hydrologic Modeling Tool have well performance in other watersheds [43,44] in extracting and bias-correction of CORDEX RCMs for hydrological modelling. Several hydrological models have been in use to model hydrological processes using spatially distributed information and time series data [45–48] under data scarce. The Soil and Water Assessment Tool (SWAT) model is implemented to quantify hydrological response and climate change studies under data scarce regions [17,18,38, 49–52] and also used in this study.

Climate change effects on hydrological response under RCMs studies are limited in this study area, but those studies conducted in the region used courser data that not favored hydrological models. Moreover, those studies conducted in this region only used single RCMs for their analysis. To understand climate change impact requires multiple ensemble average of RCMs [53]. All of the above researches were carried out at large watershed and outside the Upper Erer subbasin study area. Not any climate change anlysis studies conducted on water balance components under CORDEX RCMs on Upper Erer subbasin. Hence, quantifying climate change at subbasin level and investigating its influence on hydrological processes indicates originality of the paper. This research explains the examination of climate change projection and its effects on hydrological response from historical period (1979–2014) to future period (2024–2070) in the Upper Erer subbasin.

2. Materials and methods

2.1. Description of study area

The Upper Erer basin that drains from the Harar highlands to the Wabisheble River Basin are found at 15 km south east of Harar Town. Physically upper Erer subbasin located in between 9°13′26.4″ N to 9°31′26.4″ N latitude and 42°4′40.8″ E 42°20′38.4″ E longitude. The upper Erer river watershed area is 466 km^2 having topographical ranges of 1306–3019 m (Fig. 1).

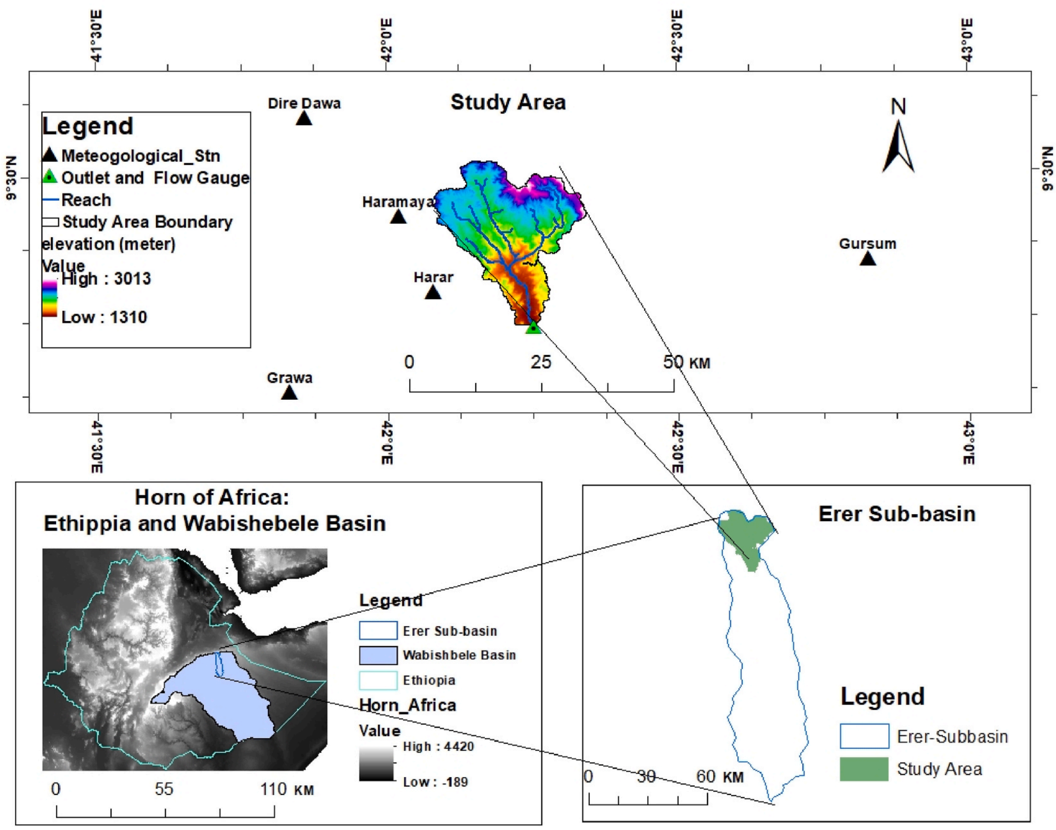

Fig. 1. Study area location.

The daily mean maximum (26.72 °C) and minimum (12.78 °C) temperatures are recorded in the region [54]. The ecological climate zone and their elevation ranges were shown in Table 1 indicates in the region the dominant agroecological zone is Woinadega (cool subhumid) [23]. The population income mostly depends on agriculture [55].

2.2. Data and methods

2.2.1. Observed climate and climate models information

National Meteorological Institute of Ethiopia (NMIE) provided the recorded precipitation information for the period (1979–2014) (Table 2). The absence of long-period of observed climatic data has significant effect on climate change impact studies [56] in data scarce regions. In Ethiopia, the long-term meteorological time-series data is a challenge, even if the country is expanding the number of meteorological stations in various parts. In the absence of ground recorded climate information the Climate Forecast System Reanalysis (CFSR) information were implemented in a data scarce condition that has good performance for various studies such as [30,40,57,58]. In this study except precipitation all other meteorological data used for SWAT model input were generated from CFSR for the period (1979–2014).

The historical and future CORDEX RCMs climate variables (precipitation, minimum and maximum) generated from CORDEX RCMs were used. The historical and projected CORDEX (RCMs RCP-4.5 and RCP-8.5 that approximately represents the medium and maximum carbon release scenarios [42,59] were selected that have been used in other studies [38,60] has good performance. To bias correct the RCMs the observed rainfall, maximum and minimum temperatures were used. It is strongly recommended by Ref. [61] to use a long overlapping period (i.e., two to three decades) for observed and original historical RCMs data. In this study two future periods were merged and produced the period (2024–2070) that used for the examination. The CORDEX dataset includes five RCMs for historical (1970–1999) and for future (2000–2099) [28]. The historical period (1979–2014) and future period (2024–2070) are considered which aligned with the water supply source for the year 2070 target.

The RCMs used in this study includes: Fourth Generation Canadian Regional Climate Model version 4 (CanRCM4), Rossby Centre Regional Atmospheric Model version 4 (RCA4), Regional Atmospheric Climate Model version 2.2 (RACMO22T), High-Resolution Hamburg Climate Model 5 (HIRAM5) and Swedish Meteorological and Hydrological Institute-Rossby Centre Regional Atmospheric Model version 4 (SMHI-RCA4). Selection of five local's climate models' information depends on broadly application in regional changing climate effects researches in Eastern Africa. Table 3 shows explanation of the RCMs information implemented in this research.

2.2.2. Extraction and bias correction

The RCMs data are not available in useable format for input in hydrological modeling. Hence, the data points were extracted by using the latitude and longitudes of stations considered. ArcGIS 10.7.1 software was employed for the extraction RCMs using NetCDF table view tool under multidimension tool of the ArcGIS interface. The RCMs information have bias due to various reasons [65,66]. The correction for bias is performed to elevate the estimation of climate model output and to minimalize the inconsistency from recorded climate variables that probably affect hydrological parameters [66,67]. The CMhyd tool were used in various application of bias-correction analysis [58,68–70]. The CMhyd tool was employed in this study to develop climate data for the SWAT model input [43,61].

The error adjustment were performed for temperatures using Equation (a) and for precipitation using Equation (b) [71].

$$T_{D,F,} = T_{RCM,Bias,D,F} + \left(meanT_{Obs,M} - meanT_{RCM,Obs,M}\right) \tag{a}$$

where, $T_{D,F,}$ is daily bias corrected climate model in projected duration, $T_{RCM,Biased,D,F}$ is daily bias raw RCM temperature in future period, and $meanT_{Obs,M}$ is mean monthly measured data in reference duration, and $meanT_{RCM,Obs,M}$ is bias mean monthly RCM in baseline period.

$$P_{D,F,} = P_{RCM,Bias,D,F}\ x \left(\left\lfloor \frac{meanP_{Obs,M}}{meanP_{RCM,Obs,M}} \right\rfloor\right) \tag{b}$$

where, $P_{D,F,}$ is daily bias corrected RCM precipitation in future period, $P_{RCM,Biased,D,F}$ is daily bias raw RCM precipitation in future period, and $meanP_{Obs,M}$ is mean monthly observed precipitation in baseline period, and $meanP_{RCM,Obs,M}$ is biased mean monthly RCM precipitation in baseline period. The ensemble average of RCMs performed well from of the discrete RCMs [36,72,73] and ensemble mean of five RCMs is used in this research.

Table 1
Ecological climate zone explanation.

Ecological climate zone types	Elevation ranges	% coverage
Warm semiarid (Kolla)	500–1500 m	13.06
Cool subhumid (Woinadega)	1500–2300 m	73.98
Cool humid (Dega)	2300–3200 m	12.96

Table 2
Description of climatological stations.

Stations name (Class category)	Physical location		Mean Elevation (m)	Mean yearly rainfall (mm)	Observation duration	Proportion of missing values (%)	Mean annual temperature	
	Latitude	Longitude					Max (°C)	Min (°C)
Dire Dawa (1st class)	9.60	41.86	1045	647	1983–2020	9.12	32.8	19.0
Haramaya (1st class)	9.43	42.02	2025	816	1983–2020	12.92	24.05	9.74
Harar (1st class)	9.30	42.08	1977	801	1985–2020	18.01	23.0	16.0
Girawa (3rd class)	9.13	41.83	2470	958	1983–2017	14.83	22.0	13.0
Gursum (3rd class)	9.35	42.39	1937	840	1983–2017	8.74	27.2	12.8

Table 3
Explanation of RCMs information.

Item	RCMs (GCMs)	Data type/sources/time span	Resolution	References
1	Can-RCM4 (Can-ESM2)	Maximum and minimum temperatures and rainfall information for references and projected periods: from CORDEX database (1979–2014) and future (2024–2070) under RCP-4.5 and 8.5	longitude 0.44° and latitude 0.44°	[37,41]
2	RCA-4 (MPI-ESM-LR)			[36,37,41,62]
3	RACMO-22T (EC-EARTH)			[27,36,62–64]
4	HIRHAM-5 (EC-EARTH)			[36,37,63,64]
5	SMHI-RCA-4 (EC-EARTH)			[59]

2.2.3. Projections analysis for climate change

Several statistical approaches are used to evaluate the implementation of regional climate models simulation [36,37]. Generated historical ensemble average RCMs of climate variables in reference duration (1979–2014) were evaluated in the study regions using observed stations. The statistical parameter used in this study is Coefficient of determination (R^2) shown equation (e). The R^2 parameters 1 indicates high value with less inconsistency, and more than 0.5 was fall under recognized ranges. Moreover, ensemble average monthly climate variables of original and bias corrected RCMs were analyzed in the reference duration for considered stations. Fig. 2 indicates summary of overall methodology and procedures used in this study.

2.2.4. Description of SWAT model arrangement and simulation

The effects of climate change on water balance components of the watershed were examined by the application of SWAT model [47] in this research. The climate change effects were detected by varying error minimized climate model information between the reference and projected duration under two emission scenarios for SWAT model input without changing other climate, spatial and temporal input data.

Table 4 shows the description of data used for SWAT model. The information for SWAT input shown in Table 4. The procedures for linking climate and hydrologic models suggested by various scholars [e.g. 74, 75, 76] have been followed for this study.

Water balance components for the SWAT model equation [47] provided in equation (c).

$$\mathrm{SW_D} = \mathrm{SW_o} + \sum_{i=1}^{t} \left(P_i - Q_{surf} - E_a - W_{Seep} - Q_{gw}\right) \quad \text{(c)}$$

Where SW_t represents final water in soil (millimeters), SW_o shows original water in soil (millimeters) on initial duration i, D represents the duration in days. While, P_i indicates rainfall in millimeters/day, Q_{surf} is the runoff in mm/day. And E_a revels the amount of evaporation and transpiration in millimeters/day, W_{Seep} represents water filtration from the soil layer in millimeters/day, and Q_{gw} represents the deep aquifer recharge in millimeters/day.

During the watershed delineation around 23 Hydraulic Response Units (HRUs) (Fig. 3 (a)) and 146 HRUs were produced for the study sub-basin. The LULC information were produced from the Landsat image information with cloud-free (<10 %), dry season and the availability of Landsat image within average time range of historical period (1979–2014).

The image classification is conducted using ArcGIS interface under supervised image classification procedures. About six land use classes are identified during the image classification (Fig. 3 (b)). The analysis of image classification accuracy was performed to identify the accuracy of the process of data generation. The soil information required for SWAT input produced from the Food and Agriculture Organization (FAO) and soil map of Ethiopia. The model databases were manually edited to make compatible with the FAO soil using database from MWSWAT of lookup table. In this process three soil group are generated (Fig. 4 (a). The model simulation uses three years warm up duration were considered as suggested by Ref. [77]. In this study DEM data were used to generate slope classes as shown in Fig. 4 (b).

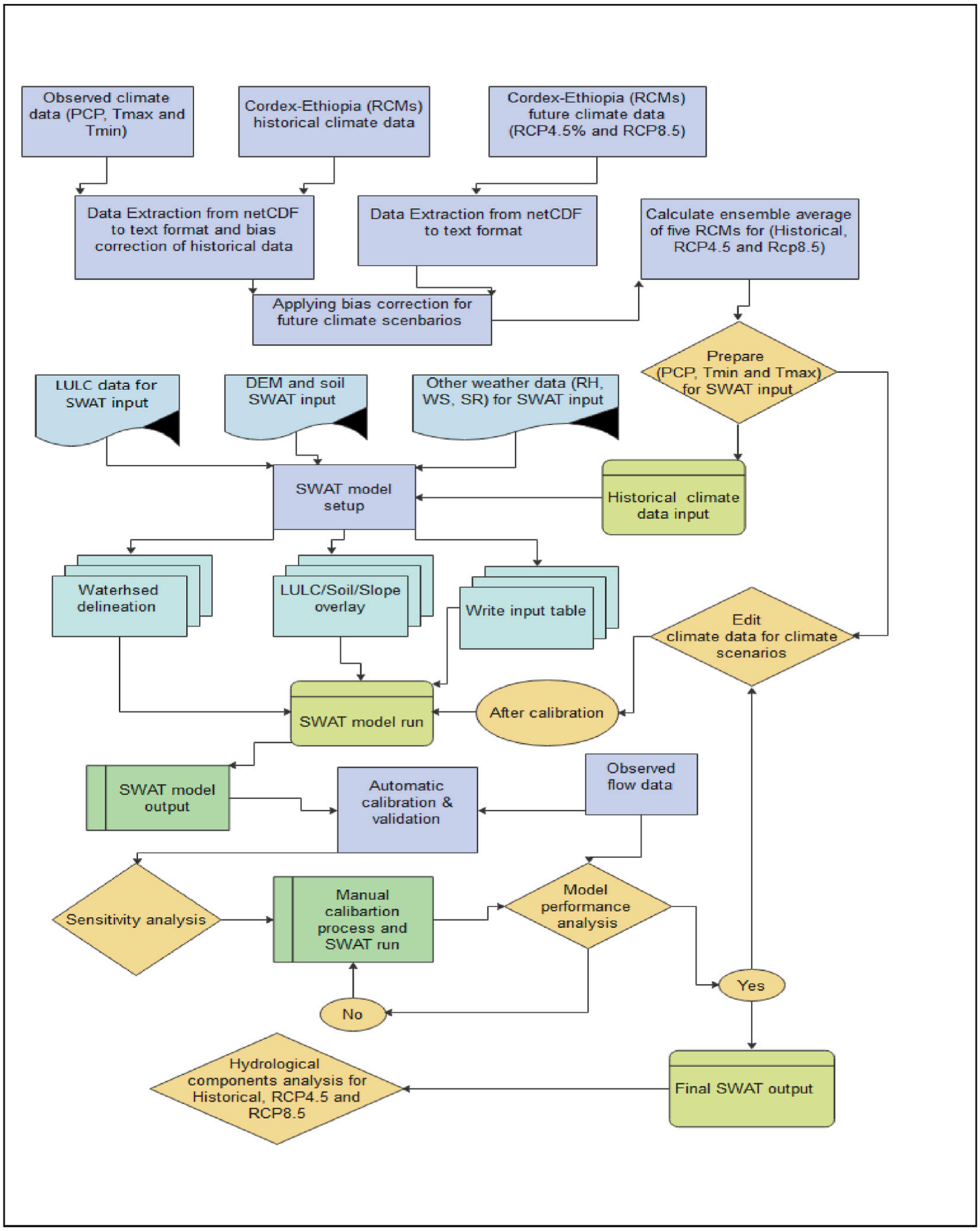

Fig. 2. Conceptual framework for the study.

2.2.5. *Hydrological model calibration and validation process*

The measured daily discharge data at outlet of upper Erer subbasin was collected. This daily discharge was transformed to monthly discharge was organized to the model input. In this research the duration (1984–1990) for calibration and (1993–1996) for validation were selected. The sensitivity analysis was implemented by employing SUFI-2 (sequential uncertainty fitting) algorithm. Were used to identify sensitive parameters form selected parameters [78]. The calibration was performed both automatically and manually [47]. In this research manual calibration and validation was also implemented [79] after automatic calibration.

2.2.6. *Investigation of sensitive parameters of hydrological model*

In the SWAT model simulation stream flow is affected by high number of parameters. The calibration of entirely these parameters at once is tedious. In this regard sensitive parameters were identified using autocalibration [49]. Initially, around seventeen flow

Table 4
Description of data used for SWAT model.

Description	Sources of data	Resolution/scale	References
Digital Elevation Model (DEM)	https://vertex.daac.asf.alaska.edu/	30 × 30 m	[51]
Land use land cover (LULC)	Landsat 7; path/row = 166/54 for year 2001 from https://www.glovis.USGS.gov	30 × 30 m	[49]
Soil data	FAO-UNESCO Global Soil Map	1:5,000,000	[49]
Recorded climate (daily data)			
Reanalysis dataset	(CFSR) (1979–2014)	0.5°x 0.5° North to South and East to west direction	[52,53]
Ground observation data: Precipitation	Ethiopian Meteorological Institute (EMI) (1979–2014)		[54]
Discharge	Ethiopian Ministry of Water and Energy (EMWE) (1984–1990) and (1993–1996)		[77]

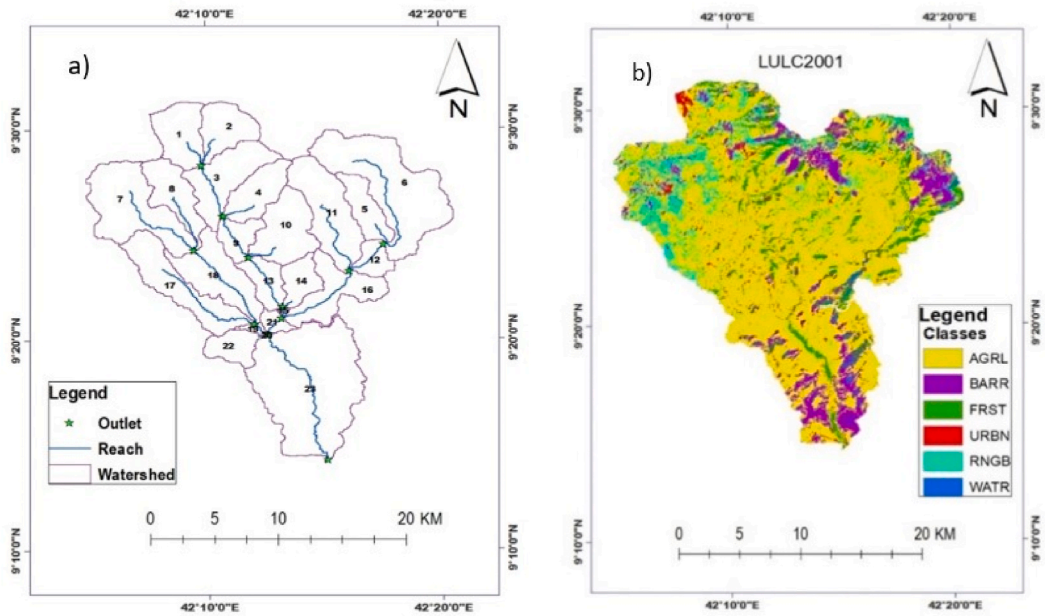

Fig. 3. Upper Errer subbasin a) Watershed delineation b) Land use land cover map.

parameters were identified form past studies. Then, employing the SUFI-2 the t stat and p values were produced. The minimum t-stat values stand for minimum sensitivity, whereas great values represent more sensitivity. Lesser p-values stands for more sensitivity, though higher values represent small sensitivity [49].

2.2.7. Performance assessment of hydrological model

The performance measures were used to assess the performance of the model in simulating observed discharge. The performance of SWAT model was evaluated by Nash–Sutcliffe efficiency (NSE), percent bias (PBIAS), and the determination coefficient (R^2) [80]. for the statistical measures Equations (d, e, and f) were used.

$$NSE = 1 - \left[\frac{\sum_{i=1}^{n}(Q_{oi} - Q_{si})^2}{\sum_{i=1}^{n}(Q_{oi} - \mathrm{Qoav})^2}\right] \tag{d}$$

$$R^2 = 1 - \left[\frac{\sum_{i=1}^{n}(Q_{oi} - Q_{sav})(Q_{oi} - Q_{oav})}{\sum_{i=1}^{n}(Q_{si} - Q_{sav})^2\sum_{i=1}^{n}(Q_{oi} - Q_{oav})^2}\right] \tag{e}$$

$$PBIAS = 1 - \left[\frac{\sum_{i=1}^{n}(Q_{oi} - Q_{si})}{\sum_{i=1}^{n}(Q_{oi})}\right] \tag{f}$$

where; Q_{oi} and Q_{si}: the measured and estimated streamflow, Q_{oav} and Q_{sav} mean of the measured and estimated streamflow.

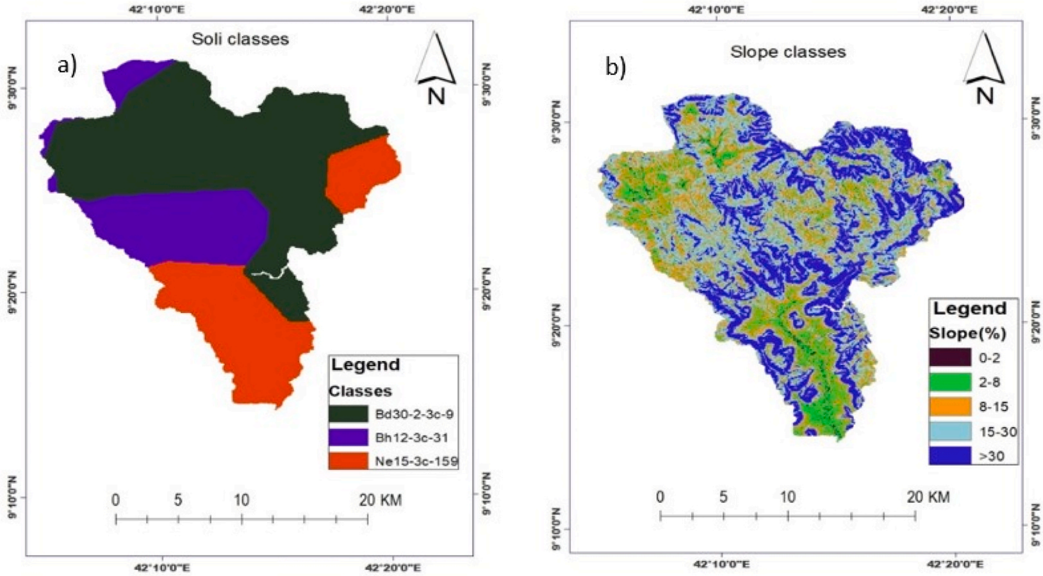

Fig. 4. Upper Errer subbasin a) Soil classes b) Slope classes.

The model is in accepted for ($R^2 \geq 0.6$), (NSE $\geq$0.5) and (-25 % $\leq$PBIAS $\geq +25$ %) according to Ref. [79]. R^2 ranges (zero to one) and as R^2 closer to one represents small discrepancy. Whereas, NSE varies from negative infinity to one with the value approach to one indicates better simulation. While, PBIAS with zero value represents better performance. The PBIAS with "+" sign standards for underestimations, while a "- "sign indicates overestimations of model output [81].

2.2.8. Evaluation of changing climate effects

The calibrated SWAT model was used to simulate future hydrological response in this research The projection of the water balance components was estimated using the calibrated SWAT model [82]. The ensemble average of bias-corrected projected period (2024–2070) of RCMs for two carbons release scenarios (RCP-4.5 and RCP-8.5) were implemented to simulate projected hydrological responses of the subbasin. The monthly and annual water balance components alteration between baseline and future duration was evaluated.

3. Results and discussion

3.1. Biased corrected RCMs assessment under baseline period

The performance of RCMS in simulating the measured climate data at a small level represents a measure for assurance in the researches of climate change effect assessment [80]. Observed climate information stands to measure model performance for bias correction output [40]. The determination coefficient used to estimate the simulation status of RCM shown in Table 5. The result indicates that for all stations the coefficient of determination statistic for average temperature were greater than 0.93. This shows the correction for bias of average temperature indicates well performance [41]. For precipitations, the determination coefficient was all >0.64 except at Haramaya station. At this station, the value is much smaller than expected. Out of five possibilities only one coefficient of determination less than 0.5 that indicates satisfactory R^2 statistics for rainfall. These indicate a good relationship between the observed and simulated monthly climate variable. Bias correction for precipitation statistics in other study shows R^2 values ranges

Table 5
Results of statistical parameters to evaluate RCMs.

Stations	Statistical parameter	
	Average temperature	Precipitation
	R^2	R^2
Dire Dawa	0.97	0.98
Girawa	0.96	0.64
Gursum	0.95	0.98
Haramaya	0.95	0.03
Harar	0.93	0.96

from 97 to 99 % [44]. In this study, bias correction can efficiently minimize errors for average rainfall except for Haramaya station.

Fig. 5(a–e) indicates ensemble mean monthly rainfall series of original and bias corrected RCMs compared with the observed in the reference duration for stations under considerations. The outcome revels original ensemble average of RCMs for precipitation series are not overlapped with the measured for entire months except (January–March) and (mid-October - December) for Dire Dawa station, (January–February) and (October–December) for Girawa station, (January–March) and (September–December) for Gursum station and (January–February) and (mid-October - December) for Harar station. But, at Haramaya station the precipitation series is not uniform throughout the year. This was perhaps associated with less effective model simulation in Haramaya gauging station or else the possibly due to its topographic characteristics during data record. After bias correction the overlap were significantly improved (Fig. 5 (a–e)).

Fig. 6(a–e) depicts the ensemble average monthly cycle of original and bias corrected RCMs compared to the mean monthly observed temperature. The original ensemble average of the RCMs for mean temperature overestimated for Girawa, Gursum and Harar stations. While, the original RCM underestimated for Dire Dawa station.

The output indicated that bias adjustment meaningfully enhanced model simulation and probably reduces the doubts happening during SWAT model running [39]. The average monthly values of ensemble average of bias corrected RCMs of temperature were

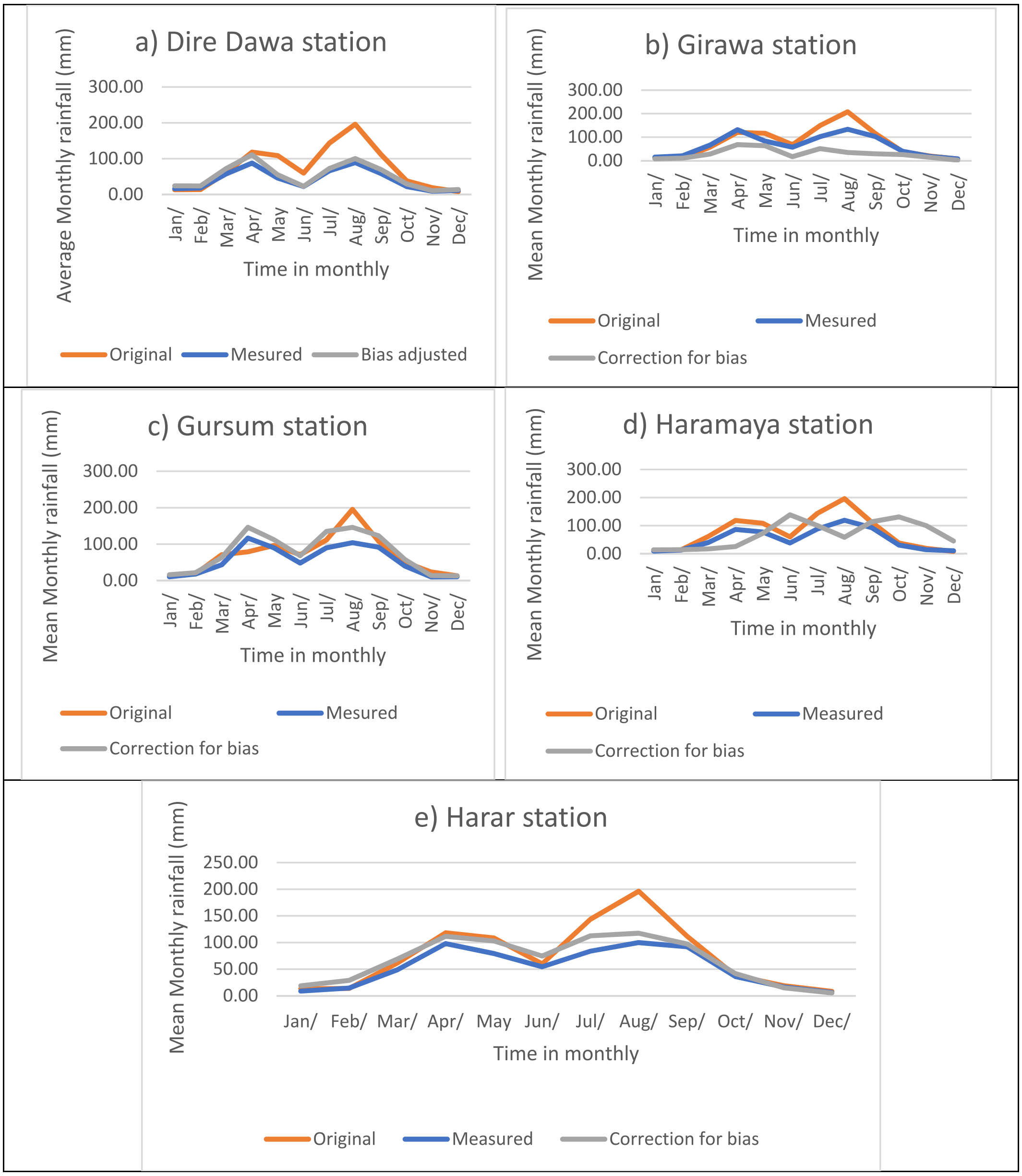

Fig. 5. (a–e). Monthly average rainfall of observed, original historical CORDEX and bias corrected historical CORDEX for the stations.

15.76 °C and 24.08 °C at Gursum and Dire Dawa stations, respectively. However, the average monthly observed mean monthly temperature was 14.59 °C and 24.88 °C at Gursum and Dire Dawa stations, respectively. At the months of August and September mean monthly ensemble average of biased corrected RCMs shows overestimation for average monthly surface temperature for all stations. But, at Haramaya station the model overestimated only for the months of October and December.

3.2. Rainfall projection analysis

Future rainfall for moderate as well as maximum carbon release scenarios were used to analyses rainfall change for the projection period (2024–2070) from reference period (1979–2014). Fig. 7(a–e) demonstrates mean monthly rainfall changes for projected period (2024–2070) for RCP-4.5 and RCP-8.5 scenarios of gauging stations. This result indicated that the future precipitation under these two scenarios will rise from May to December for Dire Dawa station, while expected to decline from January to April. At Girawa station, precipitation is expected to increase for entire months in both emission scenarios. But, projected rainfall at Gursum station expected to decrease in all months except in the months of March (RCP-8.5), June (RCP-8.5), August (RCP-4.5 as well as RCP-8.5) and November

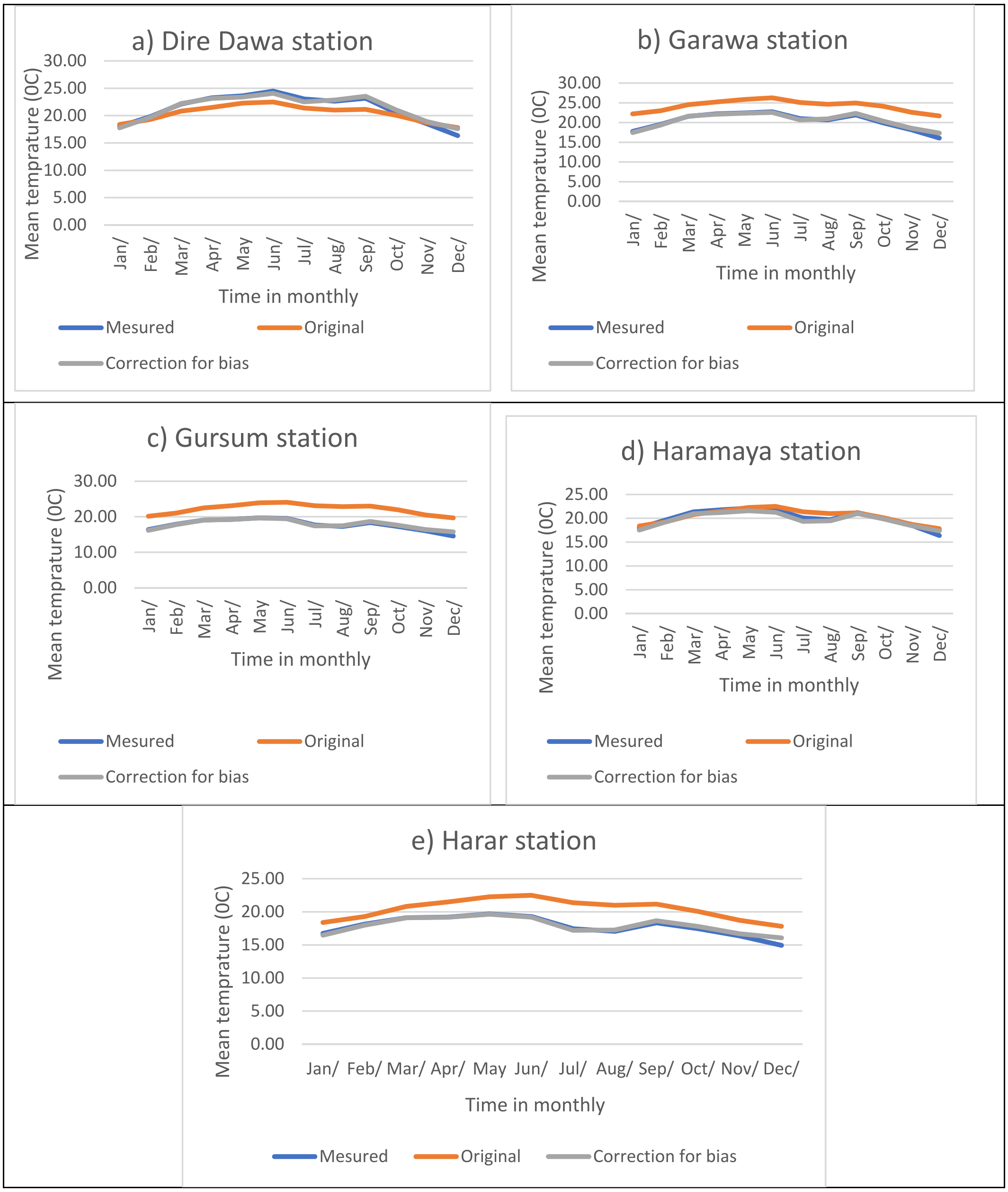

Fig. 6. (a–e). Average monthly temperature of observed, original historical CORDEX and bias corrected historical CORDEX for the stations.

(RCP-4.5 as well as RCP-8.5). At Harar and Haramaya stations, the rainfall will rise from July to September for (RCP-4.5 as well as RCP-8.5) scenarios. In general, precipitation will rise for whole stations from July to August expect at Gursum station. In The future precipitation will rise for rainy season of June, July and August at higher rate than the rest of months [83] in Dire Dawa and Girawa stations.

The output from Fig. 7(a–e) shows the rainfall projection in the Upper Erer subbasin are consistent with climate change impacts studies such as [73,84] that testifies the intra-annual rainfall change having decreasing and increasing monthly share. This indicates that rainfall changes are not uniform for all the stations [40] across the year. The maximum average monthly precipitation rise via 211.22 mm (for RCP-4.5) as well as 235.62 mm (for RCP-8.5) for the station stations. Whereas, the maximum decrease via 90.71 mm (for RCP-4.5) and 84.97 mm (for RCP-8.5). For moderate carbon release the maximum future precipitation alteration is expected at August (44.15 mm, 135.70 mm, 152.73 mm, 194.42 mm and 211.22 mm) for Gursum, Harar, Dire Dawa, Haramaya and Girawa stations, respectively. Nevertheless, the maximum future precipitation alteration is expected in the months of August (49.37 mm, 80.32 mm, 168.13 mm, 220.99 mm and 235.62 mm) for Gursum, Harar, Dire Dawa, Haramaya and Girawa stations, respectively under RCP-8.5. This indicates that the maximum changes in mean rainfall is expected to be happing in the month of August for all stations

Fig. 7. (a–e). Mean monthly rainfall change for projected (2024–2070) for RCP-4.5 and RCP-8.5.

under both scenarios. The month of August is found in wet season, having highest precipitation in the region. Projected mean rainfall change in all five stations shows the highest mean rainfall change is predictable at Girawa station, but the minimum at Gursum station.

3.3. Temperature projection analysis

The comparison the future alteration of temperatures from reference duration (1979–2014) to future duration (2024–2070) for RCP-4.5 and RCP-8.5 v was performed. Fig. 8(a–e) revels projected average monthly temperature changes for period (2024–2070) for both carbon release scenarios in reference-to-reference period (1979–2014). The outcome revealed that the increase in monthly mean temperature for RCP-8.5 is more as related to RCP-4.5 for all stations except for Haramaya station in the month of November. Whereas, the temperature for RCP-4.5 is more than for RCP-8.5 scenario.

This shows monthly average temperatures will be expected to increases [42] for projected duration in reference-to-reference duration for RCP-4.5 and RCP-8.5. The minimum alteration for average monthly temperature will rise by 0.04°C (Dire Dawa station) for RCP-4.5, while highest change in average monthly temperature be expected to rise by 6.5°C (Gursum station). Nevertheless,

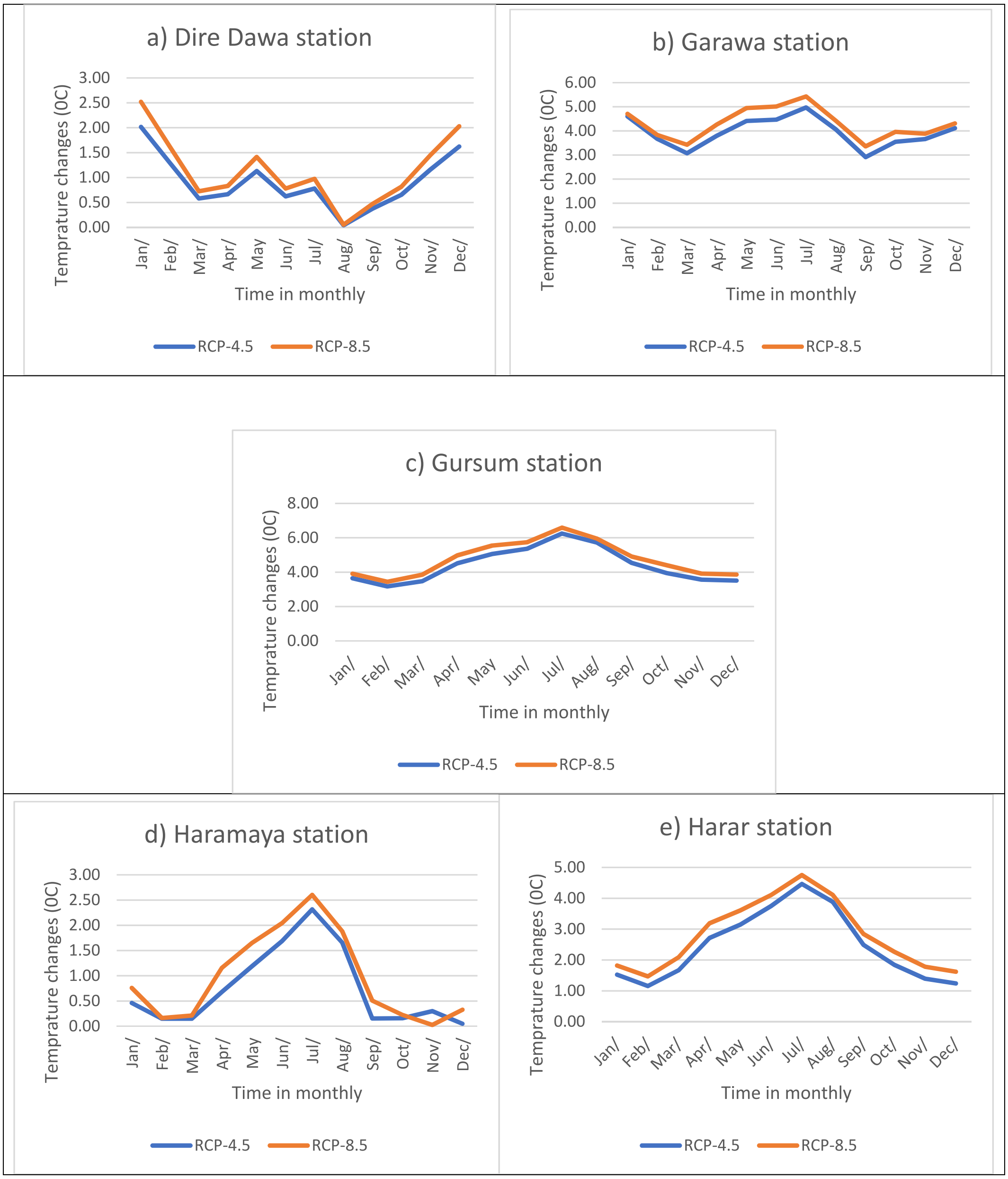

Fig. 8. (a–e). Change in mean monthly temperatures of RCP-4.5 and RCP-8.5 scenarios for five stations.

under RCP-8.5 the minimum monthly change is expected to rise by 0.03°C (Haramaya station), while the maximum mean monthly temperature change is expected to rise by 6.59 °C. This result indicates the predicted mean monthly temperature is expected to rise [85,86] for RCP-4.5 and RCP-8.5. Temperature increase is higher for RCP-8.5 than RCP-4.5 that indicates there is a high greenhouse gases concentration is expected for RCP-8.5, having a more global temperature increase. The output shows that regional environment is warmer than the current duration for RCP-4.5 and RCP-8.5 scenarios [83]. Maximum predicted average temperature change will happen for January (2.02 °C), July (4.97 °C), July (6.25 °C), July (2.32 °C) and July (4.47 °C) for Dire Dawa, Girawa, Gursum, Haramaya and Harar stations, respectively for RCP-4.5 scenarios. While, for RCP-8.5 scenario, maximum change will happen in the months of January (2.52 °C), July (2.6 °C at Dire Dawa), July (4.75 °C at Haramaya), July (5.43 ^{0}C- at Harar) and July (6.59 °C at Gursum).

The result indicates that the maximum change in aveerage temperature change will be happening in July for all stations. But for Dire Dawa station, it is expected to be happening in January. This is probably due the effect of the topographical location of Dire Dawa gauging station (lowest topography) as compared to other stations (higher topography) [Table 2]. Dire Dawa station location is categorized under warm semiarid ecological climate zone [23]. The results for future mean temperature in all five stations shows an increasing in both emission scenarios. The maximum mean temperature to be predicted for Gursum station and minimum at Dire Dawa station. Lowest projected mean temperature is expected to occur in Dire Dawa, Haramaya, Harar, Girawa and Gursum stations in increasing order under both emission scenarios. Generally, the average temperature projection in two emission scenarios is in the range that predicted by IPCC and coincides with similar studies [50,51]. Most climate change studies in various areas of Ethiopia watersheds showed that the temperature is likely to rise, such as study conducted in southwest Ethiopia [18].

3.4. Hydrological model sensitivity analysis and performance evaluation

Sensitive parameters were identified before the implementation of model simulation. Initially seventeen parameters were identified that used for sensitivity analysis by employing sufi2 algorithm in the SWATCUP model. The lowest p-value and the highest t-stat were considered to identify sensitive parameters. Using this process, ten most influential parameters were identified. Fig. 9 shows the sensitive parameters values from the autocalibration analysis.

The statistical measures NSE for calibration (0.65) and validation (0.53) found. While, R^2 for calibration (0.84) and validation (0.72) period. These showed that the model performance was well improved for calibration than the validation time. This is possibly credited to inappropriate stream flow records for the validation period or else inconsistency in hydroclimatic and spatial data. The PBIAS for calibration (−23.04 %) and validation (−14.16) for simulation indicated predicted discharge overestimated the measured discharge. Overall, statistical measures NSE, R^2 and PBIAS results shows measured and predicted monthly discharge were in good relation [81,87] as shown in [Fig. 10]. This best relation among measured and predicted discharge revels that SWAT model used to simulate monthly stream flow in the region significantly.

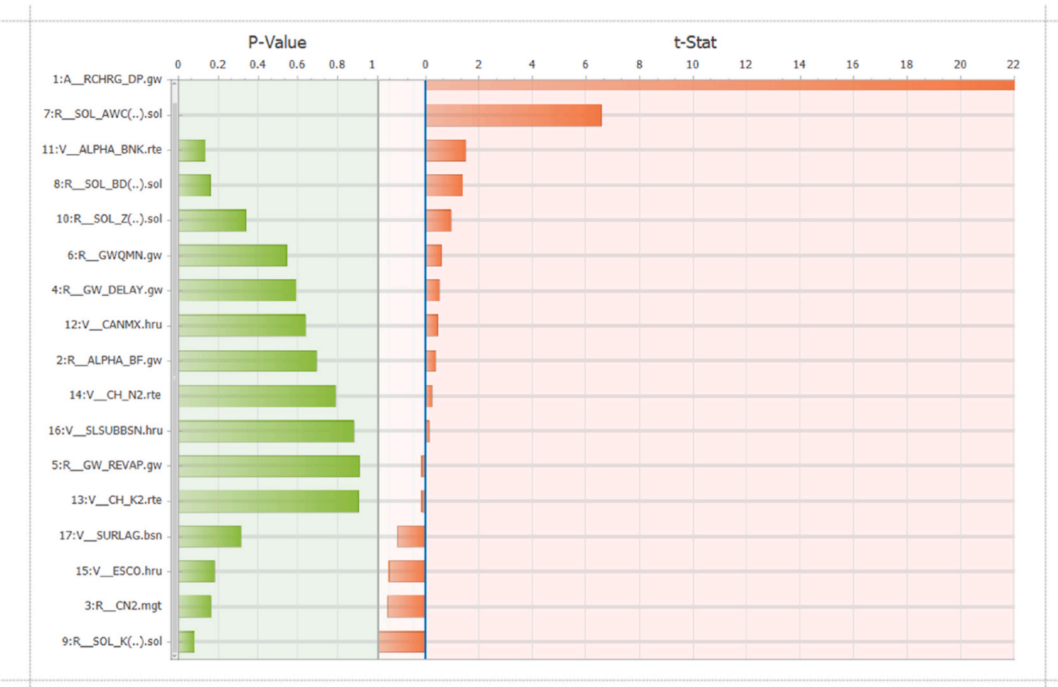

Fig. 9. Global sensitivity analysis results of parameters.

3.5. Hydrological model calibration and validation

Autocalibration and manual-calibration process were used in this study. After the autocalibration process and identification of sensitive parameters manual calibration [88] were used to adjust the SWAT model sensitive parameters. During the processes sensitive parameters were identified for groundwater and surface runoff parameters [Table 6] using the observed streamflow records. To improve the performance of the model several simulations run (twenty-eight) by adjusting the parameters values within acceptable ranges. Finally, the parameters values range and associating good match values gotten are shown in Table 6. The model simulation was performed for entire period (1979–2014) using three years warmup period (1979–1981). The calibration and validation process taken place using observed monthly stream flow for (calibration from 1984 to 1990) and (validation from 1993 to 1996).

The manual calibration process has been set in the order of sensitivity on the runoff and ground water flow parameters for instance surface CN2, GW_REVAP, REVAPMN and RCHRG_DP [88]. During first SWAT model run output shows baseflow was too low and evaporation was too high. So, adjustments were made on the groundwater flow parameters, by decreasing the GWQMN and GW-REVAP and increasing the REVAPMN parameters successively until the model performance measures were reaching satisfactory values of (NSE, R^2 and PBIAS). Then, baseflow became highest and the peak flows were lowest. Hence, adjustments were made to the surface runoff and baseflow parameters by increasing CN2 and decreasing the other flow parameters (SURLAG, ESCO and EPCO) slightly until reach reasonable statistical measures (R^2, NSE and BIAS. Then, the same adjustments were made to the soil parameters includes: Saturated hydraulic conductivity at layer 1 (SOL_K (1)), Soil water available capacity (SOL_AWC (1)) to reach the acceptable performance metrics values [49,88].

Fig. 11 (a and b) shows monthly stream flow hydrograph of (calibration and validation). The output indicates during the calibration time model overestimated (January and from April to December). Whereas, the model overestimated for the months of (April and from September to January) during validation time.

In this research peak monthly runoff was predicted for the both calibration and validation time (Fig. 11 (a and b)). Therefore, SWAT model captured the monthly peak flow at model simulation time.

This indicates, SWAT model is suitable to quantify the possible effects of change in climate as well as to understand hydrological response under refined hydro-meteorological data in the study subbasin.

3.6. Evaluation of hydrological balance variation for changing climate

The SWAT model predicted for hydrological balances of runoff, lateral flow, ground-water-flow, water-yields, evapotranspiration and potential-evapotranspiration by changing climatic variables. Climate change impacts on the hydrological balance of the upper Erer subbasin were evaluated using the temperature and rainfall changes for projected duration (2024–2070) in reference-to-reference duration (1979–2014) for RCP-4.5 and RCP-8.5 scenarios. Accordingly, Fig. 12(a–d) shows that monthly predicted change of surface-runoff lateral-flow, water-yields, evapotranspiration a potential-evapotranspiration in reference-to-reference duration RCP-4.5 and RCP-8.5. The result indicates that the projected surface runoff at (March, June, October and December) is lower under RCP-4.5 than RCP-8.5, but for the other months the surface runoff is expected to be more under RCP-4.5 than RCP-8.5. Nevertheless, lateral-flow change for entire is higher for RCP-8.5 than RCP-4.5. The water yield for entire months is expected to be lower for RCP-4.5 than RCP-8.5 excluding (May, July, October).

The mean annual change for all hydrological response shows a decrease under both emission scenarios except the potential evapotranspiration (Table 7). The monthly average flow fluctuates significantly throughout the year [42]. Hence, the predicted change in climate will decrease most of the water balance in the subbasin [83].

The SWAT model output indicates that decrease of precipitation and rise of temperatures are expected in the region. This will probably drop in surface-runoff, lateral-flow, groundwater-flow and overall water-yields. The yearly surface-flow decreases probably happening due an increase of mean temperature in the study area. This is confirmed by Ref. [44] that reported the temperature increase can result in a decrease of annual surface flow. The increment in temperature also caused an increase of Potential Evapotranspiration (PET). This shows that the temperature changes and PET are interrelated absolutely.

The result shown in Table 7 indicated that the predicted groundwater-flow to change via a higher amount and evapotranspiration

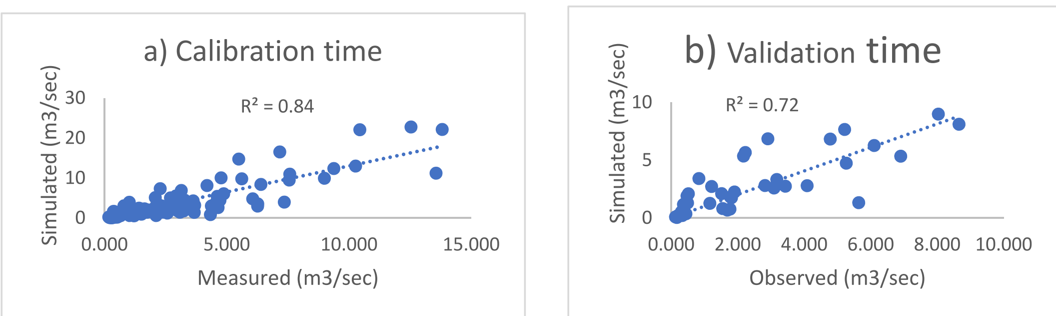

Fig. 10. Scatter plot of measured and predicted monthly streamflow for a) calibration and b) validation time.

Table 6
Fitted values for sensitive parameters in the Upper Erer subbasin.

Parameter Name	Description (unit)	Default values	Final fitted values	Min. range	Max. range
CN2_mgt	Initial-soil-conservation-service (SCS)-curve-number-2 (none)	65	72.5	35	98
SOL_AWC (1) _sol	Soil-water-available- capacity (millimeters H2O/mm soil)	0.092	0.097	0	1
SOL_K (1) _sol	Saturated-hydraulic-conductivity (millimeters/hrs.)	7.04	21.12	0	200
ESCO_hru	Soil-evaporation-compensation-factor (none)	0.95	0.92	0.01	1
EPCO_hru	Plant-uptake-compensation-factor (none)	1	0.98	0	1
GWQMN_gw	Threshold-water-level-in-shallow-aquifer-for-baseflow (millimeters)	1000	1300	0	5000
REVAPMN_gw	Threshold-depth-of-water-in-the-shallow-aquifer-for “revap.” to-occur (millimeters)	750	75	0	500
GW_REVAP_gw	Groundwater – ‘revap.’-coefficient (none)	0.02	0.018	0.02	0.2
SURLAG_bsn	Surface-runoff-lag-coefficient (none)	4	2.5	0.05	24
RCHRG_DP_gw	Deep-aquifer-percolation-fraction (none)	0.05	0.042	0	1

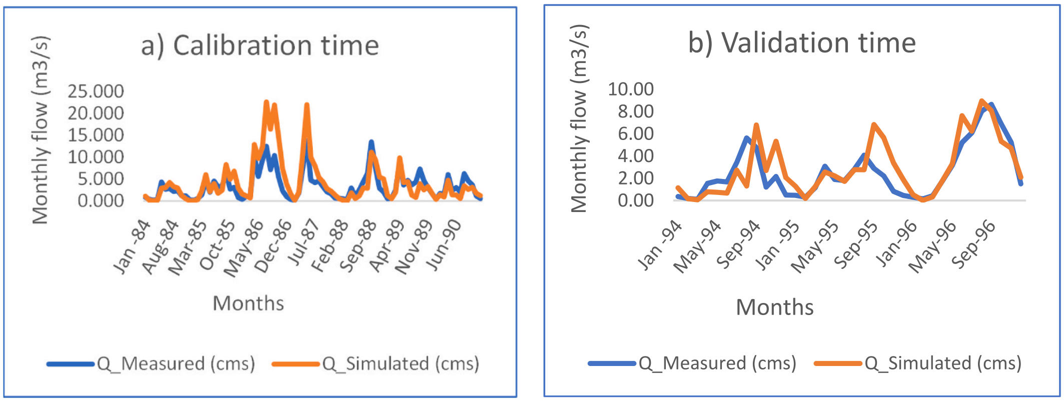

Fig. 11. Monthly runoff hydrograph for a) calibration and b) validation time.

via a minor amount. The amount change in surface runoff and lateral flow are low when compared with groundwater flow and water yield. Nevertheless, the predicted surface runoff change is higher relative to lateral-flow, water-yields, evapotranspiration and potential-evapotranspiration for both emission scenarios.

Fig. 13 shows that the mean annual projected change for RCP-4.5 and RCP-8.5 of surface-runoff, groundwater-flow, lateral-flow, water-yields, evapotranspiration and potential-evapotranspiration in reference-to-reference period. The result indicates that the highest decrease for mean annual surface runoff, ground waterflow and evapotranspiration will happen under RCP-8.5. But, the maximum decrease in mean annual water yield and lateral flow will happen under RCP-4.5. Nevertheless, the potential evapotranspiration is expected to increase under both scenario and maximum under RCP-8.5 scenario.

Generally, monthly change on water balance component will have varying intensity and surface-runoff is substantially changing than others for carbon release scenarios. However, annual climate change impacts will have maximum impacts on groundwater flow. Evapotranspiration and lateral flow are the minimum effects with the changing climate as compared to others for two scenarios. Average monthly precipitation for entire stations is variable, but at sub basin level the mean monthly rainfall is decreasing during wet season. The temperature is increasing and rainfall is decreasing (during wet season). This will decrease the surface-runoff, groundwater-flow, water-yields and evapotranspiration. While, potential-evapotranspiration will rise. The decline of mean annual water yield over the subbasin possibly will happen due to the reduction of annual and seasonal (wet season) rainfall and increasing mean surface temperatures under both emission scenarios. But station wise the mean monthly rainfall is variable. Moreover, the incline in PET will happen due to the surface temperature increases and this aggravated the decrease in rainfall and affects the ecosystem. The likely reduction of water yields critically affects the accessibility of the water resources in the region.

4. Conclusions

Eastern Ethiopia watersheds are located in transition zone from Arid to semi-humid climate. The annual rainfall distribution is highly declining in expanding westwards in the watersheds including the upper Erer subbasin. This research is focused climate change impacts assessment on future hydrological response under daily bias corrected climate variables from CORDEX RCMs on upper Erer subbasin, located in Eastern Ethiopia. The performance of ensemble average of the baseline period (1979–2014) of five RCMs was evaluated using observed climate variables. The change from the past duration (1979–2014) to future duration (2024–2070) in ensemble average of RCMs determine the predicted change in climate variables. Extraction and bias correction were performed on RCMs before using the climate data for analysis to minimize bias. It is found that the mean monthly temperature is varied from

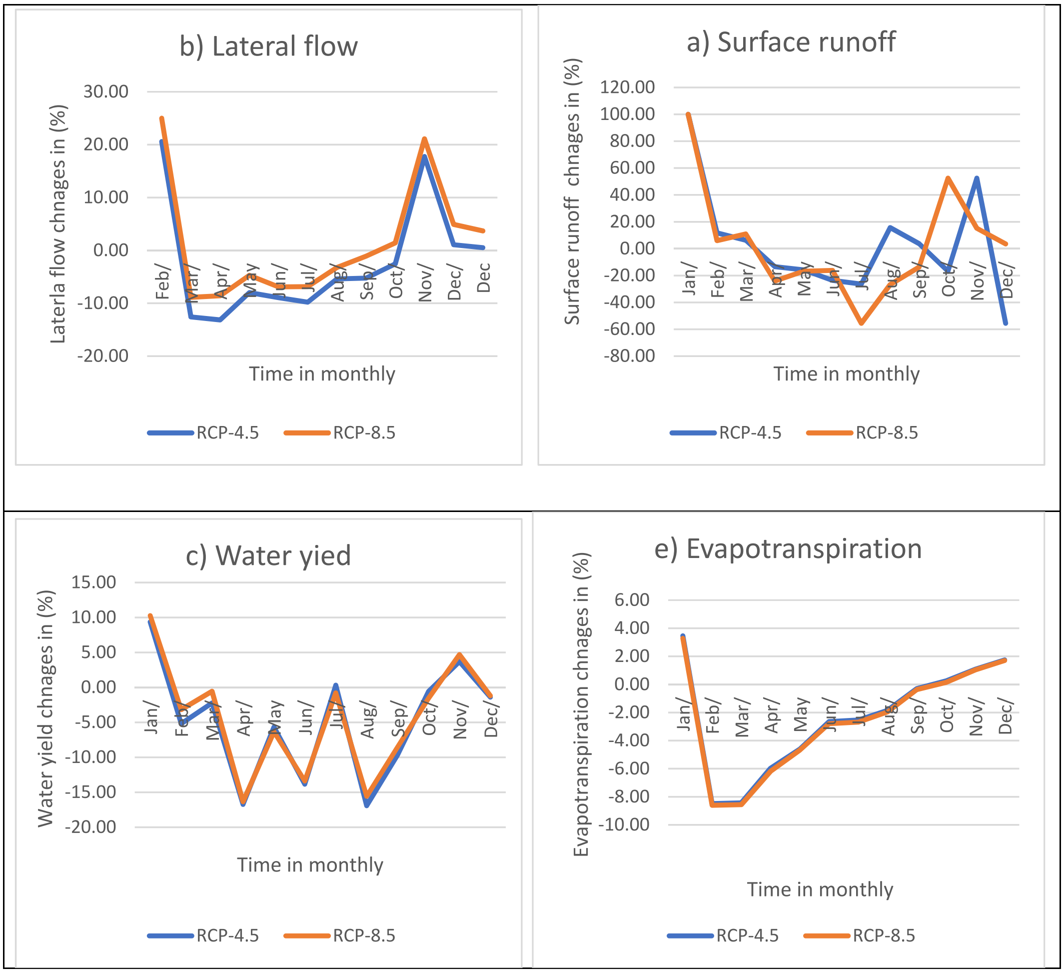

Fig. 12. (a–d). Average monthly change of predicted surface-runoff, lateral-flow, water-yields and evapotranspiration in reference-to-reference duration for RCP-4.5 and RCP-8.5.

Table 7
Annual water balance component changes for RCP-4.5 and RCP-8.5

Hydrological response (unit)	Scenarios	
	RCP-4.5	RCP-8.5
Surface runoff (%)	−4.98	−5.30
Groundwater flow (%)	−5.63	−6.68
Evapotranspiration (%)	−2.45	−2.57
Lateral flow (%)	−3.64	−0.18
Water yields (%)	−5.54	−5.21
Potential Evapotranspiration (PET)	0.47	0.49

(0.04–6.25°C) and from (0.03–6.59°C) for RCP-4.5 and RCP-8.5, respectively. However, average monthly precipitation will reduce and rises within the range of (90.71 mm–211. 22 mm) and (84.97 mm–235.62 mm) for RCP-4.5 and RCP-8.5, respectively.

SWAT model is employed to predict the hydrological balance of the reference duration and projected duration to quantify its changes. The output revels that the subbasin annual hydrological response will decrease in both scenarios having minimum value of 2.45 % (evapotranspiration) and 0.18 % (lateral-flow) and a maximum value of 5.63 % (groundwater-flow) and 6.68 % (groundwater-flow) for RCP-4.5 and RCP-8.5, respectively. The mean monthly change of streamflow is running from a maximum increase of 100 % (January) to a maximum decrease of 55.6 % (December) under both scenarios. The mean monthly changes of lateral flow with maximum increase at January (20.6 %) and maximum decrease at February (13.1 %) and having maximum increase at January (25 %) and maximum decrease at March (8.9 %) will happen for RCP-4.5 and RCP-8.5, respectively. The highest mean monthly increase and decrease in water-yields (9.4 % and 16.9 %) for RCP-4.5 scenario and (10.3 % and 16.3 %) for RCP-8.5 scenario. However, the

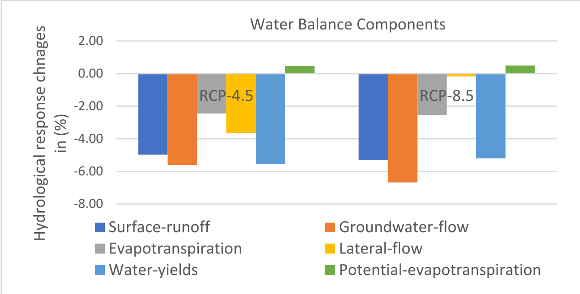

Fig. 13. Mean annual projected percentage change of surface-runoff, groundwater-flow, evapotranspiration, lateral-flow, water-yield and potential-evapotranspiration for RCP-4.5 and RCP-8.5 scenarios in reference-to-reference duration.

maximum average monthly evapotranspiration increase (3.5 % and 3.33 %) and maximum decrease (8.5 % and 8.6 %) for RCP-4.5 and RCP-8.5 scenarios, respectively. The hydrological components vary significantly for all the months in the year and high values is expected to happen in (November, December and January) that concedes with dry season. While, lowest hydrological response change is expected in (March, April, May, June and August) that fall under wet season in the region. Moreover, the decreasing hydrological response is expected to be happening in the wet season (from March to July). But, surface-runoff is increasing in March only.

In general, the climate model prediction demonstrates high variation in model performance for one station. This is therefore, it is crucial to identify these deviations to examine change in climate effects on water sources systems. In addition, hydrological model simulation process indicates that the model prediction was better at calibration than validation time. This is probably due to poor quality of stream flow records and inconsistency in hydroclimatic and spatial data. Hence, future research may use refined hydrometric and spatial data for reasonable result.

Funding

This research received no external funding.

CRediT authorship contribution statement

Bedasa Abrahim Mummed: Writing – review & editing, Writing – original draft, Visualization, Validation, Supervision, Software, Resources, Project administration, Methodology, Investigation, Formal analysis, Data curation, Conceptualization. **Yilma Seleshi:** Writing – review & editing.

Declaration of competing interest

The authors declares that there are no conflicts of interest to declare.

Acknowledgments

Acknowledgements were to the National Meteorological Institute and the Ministry of Water and Energy of Ethiopia for providing the data.

Appendix A. Supplementary data

Supplementary data to this article can be found online at https://doi.org/10.1016/j.heliyon.2024.e30297.

References

[1] Brij Kishor Pandey, Deepak Khare, Identification of trend in long term precipitation and reference evapotranspiration over Narmada River basin (India), Global Planet. Change 161 (2018) 172–182.
[2] A.B. Dariane, E. Pouryafar, Quantifying and projection of the relative impacts of climate change and direct human activities on streamflow fluctuations, Climatic Change 165 (1–2) (2021) 34.
[3] IPCC-AR6, AR6 Climate Change 2021: the Physical Science Basis, 2021. https://www.ipcc.ch/report/ar6/wg1/downloads/report/IPCC_AR6_WGI_TS.
[4] Rajendra K. Pachauri, et al., Climate change 2014: synthesis report. Contribution of working groups I, II and III to the fifth assessment report of the intergovernmental panel on climate change, Ipcc (2014).
[5] Sunitha Koneti, Sri Lakshmi Sunkara, Parth Sarathi Roy, Hydrological modeling with respect to impact of land-use and land-cover change on the runoff dynamics in Godavari River Basin using the HEC-HMS model, ISPRS Int. J. Geo-Inf. 7 (6) (2018) 206.

[6] Parisa Sadat Ashofteh, Omid Bozorg Haddad, Miguel A. Mariño, Climate change impact on reservoir performance indexes in agricultural water supply, J. Irrigat. Drain. Eng. 139 (2) (2013) 85–97.
[7] Parisa Sadat Ashofteh, Omid Bozorg Haddad, Miguel A. Mariño, Scenario assessment of streamflow simulation and its transition probability in future periods under climate change, Water Resour. Manag. 27 (2013) 255–274.
[8] Firoozeh Azadi, Parisa-Sadat Ashofteh, Xuefeng Chu, Evaluation of the effects of climate change on thermal stratification of reservoirs, Sustain. Cities Soc. 66 (2021) 102531.
[9] Seyedeh Hadis Moghadam, Parisa-Sadat Ashofteh, Hugo A. Loáiciga, Application of climate projections and Monte Carlo approach for assessment of future river flow: Khorramabad River Basin, Iran, J. Hydrol. Eng. 24 (7) (2019) 05019014.
[10] Parisa-Sadat Ashofteh, Omid Bozorg-Haddad, Hugo A. Loáiciga, Development of adaptive strategies for irrigation water demand management under climate change, J. Irrigat. Drain. Eng. 143 (2) (2017) 04016077.
[11] Parisa-Sadat Ashofteh, Taher Rajaee, Parvin Golfam, Assessment of water resources development projects under conditions of climate change using efficiency indexes (EIs), Water Resour. Manag. 31 (12) (2017) 3723–3744.
[12] P. Golfam, P.S. Ashofteh, H.A. Loáiciga, "Modeling adaptation policies to increase the synergies of the water-climate-agriculture nexus under climate change, Environ. Dev. 37 (2021) 100612.
[13] Parvin Golfam, Parisa-Sadat Ashofteh, Performance indexes analysis of the reservoir-hydropower plant system affected by climate change, Water Resour. Manag. 36 (13) (2022) 5127–5162.
[14] Seyedeh Hadis Moghadam, Parisa-Sadat Ashofteh, Hugo A. Loáiciga, Investigating the performance of data mining, lumped, and distributed models in runoff projected under climate change, J. Hydrol. 617 (2023) 128992.
[15] Seyedeh Hadis Moghadam, Parisa-Sadat Ashofteh, Hugo A. Loáiciga, ''Use of surface and groundwater under climate-change: Khoramabad basin, Iran.'', in: Proceedings of the Institution of Civil Engineers-Water Management, vol. 176, Thomas Telford Ltd, 2023. No. 2.
[16] Parisa-Sadat Ashofteh, et al., Applying climate adaptation strategies for improvement of management indexes of a river–reservoir irrigation system, Irrigat. Drain. 68 (3) (2019) 420–432.
[17] Mulugeta Musie, Sumit Sen, Indrajeet Chaubey, Hydrologic responses to climate variability and human activities in Lake Ziway Basin, Ethiopia, Water 12 (1) (2020) 164.
[18] Tesfaye Dessu Geleta, et al., Downscaled climate change projections in urban centers of Southwest Ethiopia using CORDEX Africa simulations, Climate 10 (10) (2022) 158.
[19] Fikru Abiko Anose, et al., Spatio-temporal hydro-climate variability in Omo-Gibe River Basin, Ethiopia, Clim. Serv. 24 (2021) 100277.
[20] Urszula Somorowska, Climate-driven changes to streamflow patterns in a groundwater-dominated catchment, Acta Geophys. 65 (4) (2017) 789–798.
[21] Michael O. Dioha, Kumar Atul, Exploring greenhouse gas mitigation strategies for agriculture in Africa: the case of Nigeria, Ambio 49 (9) (2020) 1549–1566.
[22] G.G. Cherie, A. Fentaw, Climate Change Impact Assessment of Dire Dam Water Supply, AAUCED HES, Ethiopia, 2015.
[23] Ministry of Agriculture (MOA), Agroecological Zones of Ethiopia: Addis Ababa, Ethiopia, 2000.
[24] Harar Water Supply and Sewerage Authority (HWSSA), Evaluation of Groundwater Resource Potential of Upper Errer Valley by Geo-Engineering Service, 2014.
[25] Yong Chen, et al., Spatio-temporal analysis of historical and future climate data in the Texas high plains, Sustainability 12 (15) (2020) 6036.
[26] Kenneth D. Frederick, David C. Major, Eugene Z. Stakhiv (Eds.), Climate Change and Water Resources Planning Criteria, Springer Science & Business Media, 2013.
[27] Bryson Bates, Zbigniew Kundzewicz, Shaohong Wu, Climate Change and Water, Intergovernmental Panel on Climate Change Secretariat, 2008.
[28] R.L. Wilby, P.J. Wood, Introduction to adapting water management to climate change: putting our science into practice, Area 44 (4) (2012) 394–399.
[29] K. Abdo, B. Fiseha, T. Rientjes, A. Gieske, A. Haile, Assessment of climate change impacts on the hydrology of Gilgel Abay catchment in Lake Tana basin, Ethiopia, Hydrol. Process. 23 (2009) 3661–3669.
[30] Dile, Y.T., Srinivasan, R. Evaluation of CFSR climate data for hydrologic prediction in data-scarce watersheds: an application in the blue nile river basin. J. Am. Water Resour. Assoc. 50 (5), 1226–1241. doi:10.1111/jawr.12182.
[31] IPCC 2013, Climate change: the physical science basis, in: T. Stoker, D. Qin, K. Lattner, M. Tigner, K. Allen, J. Boschung, A. Nauels, Y. Xia, V. Bex (Eds.), Contribution of Working Group I to the Fifth Assessment Report of the Intergovernmental Panel on Climate Change, Cambridge University Press, Cambridge, UK, 2013.
[32] Filippo Giorgi, Colin Jones, Ghassem R. Asrar, Addressing climate information needs at the regional level: the CORDEX framework, World Meteorol. Organ. Bull. 58 (3) (2009) 175.
[33] Grigory Nikulin, et al., Precipitation climatology in an ensemble of CORDEX-Africa regional climate simulations, J. Clim. 25 (18) (2012) 6057–6078.
[34] Jr Gutowski, J. William, et al., WCRP Coordinated Regional Downscaling Experiment (CORDEX): a Diagnostic MIP for CMIP6, 2016.
[35] Gebrekidan Worku, et al., Evaluation of regional climate models performance in simulating rainfall climatology of Jemma sub-basin, Upper Blue Nile Basin, Ethiopia, Dynam. Atmos. Oceans 83 (2018) 53–63.
[36] Wakjira T. Dibaba, Konrad Miegel, Tamene A. Demissie, Evaluation of the CORDEX regional climate models performance in simulating climate conditions of two catchments in Upper Blue Nile Basin, Dynam. Atmos. Oceans 87 (2019) 101104.
[37] Tamene Adugna Demissie, Chala Hailu Sime, Assessment of the performance of CORDEX regional climate models in simulating rainfall and air temperature over southwest Ethiopia, Heliyon 7 (8) (2021) e07791.
[38] Alessandro Dosio, et al., Dynamical downscaling of CMIP5 global circulation models over CORDEX-Africa with COSMO-CLM: evaluation over the present climate and analysis of the added value, Clim. Dynam. 44 (2015) 2637–2661.
[39] Salih Duri Abdulahi, et al., Response of climate change impact on streamflow: the case of the Upper Awash sub-basin, Ethiopia, J. Water Clim. Change 13 (2) (2022) 607–628.
[40] Kofi A. Yeboah, et al., Assessing climate change projections in the Volta Basin using the CORDEX-Africa climate simulations and statistical bias-correction, Environ. Challenges 6 (2022) 100439.
[41] Yonas Mathewos, Brook Abate, Mulugeta Dadi, "Performance of the CORDEX-Africa Regional Climate Model in capturing precipitation and air temperature conditions in the Omo Gibe River Basin, Ethiopia." (2022).
[42] Tufa Feyissa Negewo, Arup Kumar Sarma, Evaluation of climate change-induced impact on streamflow and sediment yield of Genale watershed, Ethiopia. The Nature, Causes, Effects and Mitigation of Climate Change on the Environment, IntechOpen, 2021.
[43] H. Rathjens, et al., "Documentation for preparing simulated climate change data for hydrologic impact studies." (2016) swat. tamu. edu/software/cmhyd.
[44] B. Zhang, N.K. Shrestha, P. Daggupati, R. Rudra, R. Shukla, B. Kaur, J. Hou, Quantifying the impacts of climate change on streamflow dynamics of two major rivers of the Northern lake Erie basin in Canada, Sustainability 10 (2018) 2897 [CrossRef].
[45] Christoph Schurz, et al., A comprehensive sensitivity and uncertainty analysis for discharge and nitrate-nitrogen loads involving multiple discrete model inputs under future changing conditions, Hydrol. Earth Syst. Sci. 23 (3) (2019) 1211–1244.
[46] F.H.S. Chiew, J. Vaze, Hydrologic nonstationarity and extrapolating models to predict the future: overview of session and proceeding, Proc. Int. Assoc. Hydrol. Sci. 371 (2015) 17–21, 371.
[47] Jeffrey G. Arnold, et al., Large area hydrologic modeling and assessment part I: model development 1, JAWRA J. Am. Water Resour. Assoc. 34 (1) (1998) 73–89.
[48] Charles Onyutha, Influence of hydrological model selection on simulation of moderate and extreme flow events: a case study of the Blue Nile basin, Adv. Meteorol. 2016 (2016).
[49] S.A. Vaghef, K.C. Abbaspour, M. Faramarzi, R. Srinivasan, J.G. Arnold, Modeling crop water productivity using a coupled SWAT-MODSIM model, Water 9 (2017) 157.
[50] Charles Gyamfi, Julius Musyoka Ndambuki, Ramadhan Wanjala Salim, Application of SWAT model to the Olifants Basin: calibration, validation and uncertainty analysis, J. Water Resour. Protect. 8 (3) (2016) 397.

[51] Q. Zhao, et al., Impact of changes in land use and climate on the runoff based on SWAT model in dawen River Basin, China, Appl. Ecol. Environ. Res. 17 (2019) 2.
[52] Darren L. Ficklin, et al., Climate change sensitivity assessment of a highly agricultural watershed using SWAT, J. Hydrol. 374 (1–2) (2009) 16–29.
[53] Jugwon Kim, et al., Evaluation of the CORDEX-Africa multi-RCM hindcast: systematic model errors, Clim. Dynam. 42 (2014) 1189–1202.
[54] National Meteorological Agency (NMA), Mean Monthly Rainfall Data; NMA: Addis Ababa, Ethiopia, 2015.
[55] Yeneayehu Fenetahun Mihertu, Over view of socio-economic data on eastern Ethiopia region (harar biodiversity center working zone), Acta Sci. Agric. 3 (2019) 196–206.
[56] Hussen Seid Endris, et al., Teleconnection responses in multi-GCM driven CORDEX RCMs over Eastern Africa, Clim. Dynam. 46 (2016) 2821–2846.
[57] D.R. Fuka, M.T. Walter, C. Macalister, A.T. Degaetano, T.S. Steenhuis, Z.M. Easton, Using the climate forecast system reanalysis as weather input data for watershed models, Hydrol. Process. 28 (22) (2014) 5613–5623, https://doi.org/10.1002/hyp.10073.
[58] Carolyne WL. Andrade, et al., Climate change impact assessment on water resources under RCP- scenarios: a case study in Mundaú River Basin, Northeastern Brazil, Int. J. Climatol. 41 (2021) E1045–E1061.
[59] Stefan Liersch, et al., Bias-corrected CORDEX precipitation, min/mean/max temperature for Ethiopia, RCP 4.5 and RCP 8.5. https://doi.org/10.5880/PIK.2018.009, 2018.
[60] Mou Leong Tan, et al., Impacts and uncertainties of climate change on streamflow of the Johor River Basin, Malaysia using a CMIP5 general circulation model ensemble, J. Water Clim. Change 5 (4) (2014) 676–695.
[61] Eshetu Zewdu, Gebre Hadgu, Lisanework Nigatu, Impacts of climate change on sorghum production in North Eastern Ethiopia, Afr. J. Environ. Sci. Technol. 14 (2) (2020) 49–63.
[62] Latifa O. Nyembo, et al., Historical and projected spatial and temporal rainfall status of Dar es Salaam, Tanzania, from 1982 to 2050, Front. Environ. Sci. 10 (2022) 2442.
[63] Giuseppe Mascaro, et al., Performance of the CORDEX-Africa regional climate simulations in representing the hydrological cycle of the Niger River basin, J. Geophys. Res. Atmos. 120 (24) (2015) 12425–12444.
[64] Bekan Chelkeba Tumsa, Statistical Evaluation of RCM's Performances in Simulation of Climate Variables at Upper Awash Basin, Case Study of Akaki Catchment, 2021.
[65] Bettina Schaefli, Projecting hydropower production under future climates: a guide for decision-makers and modelers to interpret and design climate change impact assessments, Wiley Interdiscip. Rev.: Water 2 (4) (2015) 271–289.
[66] L. Phil Graham, Johan Andréasson, Bengt Carlsson, Assessing climate change impacts on hydrology from an ensemble of regional climate models, model scales and linking methods–a case study on the Lule River basin, Climatic Change 81 (Suppl 1) (2007) 293–307.
[67] Wakjira Takala Dibaba, Tamene Adugna Demissie, Konrad Miegel, Watershed hydrological response to combined land use/land cover and climate change in highland Ethiopia: Finchaa catchment, Water 12 (6) (2020) 1801.
[68] Peipei Tian, et al., Large decrease in streamflow and sediment load of Qinghai–Tibetan Plateau driven by future climate change: a case study in Lhasa River Basin, Catena 187 (2020) 104340.
[69] De Carvalho, Juliana Wilse Landolfi Teixeira, Isabela Raquel Ramos Iensen, Irani dos Santos, Resilience of Hydrologic Similarity Areas to extreme climate change scenarios in an urban watershed, Urban Water J. 18 (10) (2021) 817–828.
[70] Geert Lenderink, Adri Buishand, Willem Van Deursen, Estimates of future discharges of the river Rhine using two scenario methodologies: direct versus delta approach, Hydrol. Earth Syst. Sci. 11 (3) (2007) 1145–1159.
[71] Claudia Teutschbein, Seibert Jan, Bias correction of regional climate model simulations for hydrological climate-change impact studies: review and evaluation of different methods, J. Hydrol. 456 (2012) 12–29.
[72] Claudia Teutschbein, et al., Regional climate models for hydrological impact studies at the catchment scale: a review of recent modeling strategies, Geogr. Compass 4 (7) (2010) 834–860.
[73] T. Gadissa, M. Nyadawa, F. Behulu, B. Mutua, The effect of climate change on loss of lake volume: case of sedimentation in Central Rift Valley, Hydrology 5 (2018) 67.
[74] Thomas Lafon, et al., Bias correction of daily precipitation simulated by a regional climate model: a comparison of methods, Int. J. Climatol. 33 (6) (2013) 1367–1381.
[75] R. Hendrik, et al., Documentation for preparing simulated climate change data for hydrologic impact studies, CMhyd User Man. (2016).
[76] Ram P. Neupane, Joseph D. White, E. Alexander Sara, Projected hydrologic changes in monsoon-dominated Himalaya Mountain basins with changing climate and deforestation, J. Hydrol. 525 (2015) 216–230.
[77] C.C. Balascio, D.J. Palmeri, H. Gao, Use of a genetic algorithm and multi-objective programming for calibration of a hydrologic model, Trans. ASAE 41 (3) (1998) 615.
[78] Karl E. Taylor, Summarizing multiple aspects of model performance in a single diagram, J. Geophys. Res. Atmos. 106 (D7) (2001) 7183–7192.
[79] Daniel N. Moriasi, et al., Model evaluation guidelines for systematic quantification of accuracy in watershed simulations, Trans. ASABE 50 (3) (2007) 885–900.
[80] Brian Ayugi, et al., Evaluation and projection of mean surface temperature using CMIP6 models over East Africa, J. Afr. Earth Sci. 181 (2021) 104226.
[81] Daniel N. Moriasi, et al., Hydrologic and water quality models: performance measures and evaluation criteria, Trans. ASABE 58 (6) (2015) 1763–1785.
[82] Hailu Gisha Kuma, Fekadu Fufa Feyessa, Tamene Adugna Demissie, Hydrologic responses to climate and land-use/land-cover changes in the Bilate catchment, Southern Ethiopia, J. Water Clim. Change 12 (8) (2021) 3750–3769.
[83] Jamal Hassan Ougahi, Shahid Karim, Syed Amer Mahmood, Application of the SWAT model to assess climate and land use/cover change impacts on water balance components of the Kabul River Basin, Afghanistan, J. Water Clim. Change 13 (11) (2022) 3977–3999.
[84] Mekonnen H. Daba, You Songcai, Assessment of climate change impacts on river flow regimes in the upstream of Awash Basin, Ethiopia: based on IPCC fifth assessment report (AR5) climate change scenarios, Hydrology 7 (4) (2020) 98.
[85] B.T. Kassie, R.P. Rotter, H. Hengsduk, S. Asseng, M.K. Vanittersum, H. Kahiluoto, H. Van Keulen, Climate variability and change in the Central Rift Valley of Ethiopia: challenges for rainfed crop production, J. Agric. Sci. (2013) 1–17, https://doi.org/10.1017/S0021859612000986.
[86] A. Kebede, B. Diekkruger, S.A. Moges, An assessment of temperature and precipitation change projections using a regional and a global climate model for the Baro-Akobo Basin, Nile Basin, Ethiopia, J. Earth Sci. Climatic Change 4 (133) (2013) 1–12, https://doi.org/10.4172/2157-7617.1000133.
[87] Sarah Osima, et al., Projected climate over the greater Horn of Africa under 1.5 C and 2 C global warming, Environ. Res. Lett. 13 (6) (2018) 065004.
[88] S.L. Neitsch, J.G. Arnold, J.R. Kiniry, J.R. Williams, Soil & Water Assessment Tool Theoretical Documentation Version 2009; Texas Water Resources Institute Technical Report No.406, Texas A&M University System, College Station, TX, USA, 2011. Available online: https://swat.tamu.edu/media/99192/swat2009-theory.pdf. (Accessed 23 February 2020).